Solubilization properties and structural characterization of dissociated HgO and $HgCl_2$ in deep eutectic solvents

Valentina Migliorati,*[a] Giuseppe Fazio,[a] Simone Pollastri,[b] Alessandra Gentili,
[a] Pierpaolo Tomai,[a] Francesco Tavani,[a] Paola D'Angelo,*[a]

[a] *Dipartimento di Chimica, Università di Roma "La Sapienza", P. le A. Moro 5, 00185 Roma, Italy*
[b] *Sincrotrone Trieste S.C.p.A s.s. 14, km 163.5, I-34149 Basovizza, Trieste, Italy*

Abstract

A synergic approach combining X-ray absorption near-edge structure (XANES) and extended X-ray absorption fine structure (EXAFS) spectroscopies together with quantum mechanical (QM) calculations on cluster models has been used to investigate the solvation properties of the $HgCl_2$ salt and HgO dissolved in deep eutectic solvents (DESs). Choline chloride (ChCl)-based DESs were prepared using different hydrogen bond donors, namely 1:2 mixtures of ChCl and either urea, acetylsalicylic acid (ASA) or sesamol (SES) and a 1:1 mixture of ChCl and pyrogallol (PYR). The XANES results show that both $HgCl_2$ and HgO molecules are completely dissociated in all the investigated DESs and the Hg^{2+} first coordination shell is composed only of Cl^- anions in all the systems, with a local structure of Cl^- ligands around the Hg^{2+} ion that is the same independently of the DES solvent and of the nature of the dissolved species. By applying a deconvolution procedure on the Hg L_3-edge raw XANES experimental data and carrying out fitting procedures of the deconvolved XANES data using different coordination models for the Cl^- anions surrounding Hg^{2+}, we were able to unambigously determine the coordination number and the geometry of the Hg^{2+} first shell complex, namely a $[HgCl_4]^{2-}$ tetrahedral coordination model. The analysis of the EXAFS spectra of $HgCl_2$ salt in ChCl-Urea, ChCl-ASA, ChCl-SES and ChCl-PYR and of HgO dissolved in ChCl-ASA allowed us to obtain a very accurate determination of the Hg-Cl first shell average distance (2.47-2.48 Å), in agreement with the XANES determinations. Moreover, ab initio calculations of different $[HgCl_n]^{(2-n)+}$ clusters carried out both in vacuum and simulating bulk solvent effects by means of the SMD solvation model strongly support the experimental findings that, in DESs, Hg^{2+} forms a complex with four chloride ions arranged in a tetrahedral geometry. The Cl^- ion is thus shown to form such strong interactions with Hg^{2+} that none of the DES hydrogen bond donors is able to compete with it and act as a ligand for Hg^{2+}. The strong solvation ability of the Cl^- anions towards metal ions can be at the origin of the high solubility of metal oxides in chloride-based DESs, which is crucial in several important processes such as metal winning, corrosion remediation and catalyst preparation.

Keywords: Deep eutectic solvents, metal oxides, mercury, EXAFS, XANES, ab initio calculations

1. Introduction

The processing and reprocessing of metals has one of the largest energy costs in industry and it is also one of the largest sources of low grade waste. Metal processing is in general rather complex due to the presence of many different starting materials, such as oxides, silicates or alloys and it is particularly challenging in the case of metal oxides, since they are insoluble in most molecular solvents and often can be only solubilized in high temperature molten salts or in aqueous acid or alkali media. Both methods have considerable disvantages regarding energy demand and waste. However, the dissolution of metal oxides is crucial in several important processeses such as metal winning, corrosion remediation and catalyst preparation and, for this reason, there has been a growing interest in developing different procedures. Ionic liquids (ILs) have been investigated for metal processing in a number of works,[1, 2, 3, 4, 5, 6] but given the cost and sustainability of these solvents, cheaper alternatives are needed for large scale applications. Abbott et al. introduced an innovative class of solvents,[7] the so-called deep eutectic solvents (DESs), which could be potential alternatives to ILs,[8, 9, 10, 11] thanks to their capability to dissolve a wide range of metal oxides.[12, 13, 14, 15] DESs are mixtures of a salt and one or more hydrogen bond donors having a melting point significantly lower than that of each individual component. In the last decade DESs are receiving an increasing attention as they show many interesting properties similar to those of ILs,[16, 17, 18, 19, 20, 21, 22, 23, 24] being at the same time less expensive, more synthetically accessible, non-toxic, and biodegradable.

Mercury is one of the most toxic metals and represents a sig-

Email address:
valentina.migliorati@uniroma1.it,p.dangelo@uniroma1.it ()

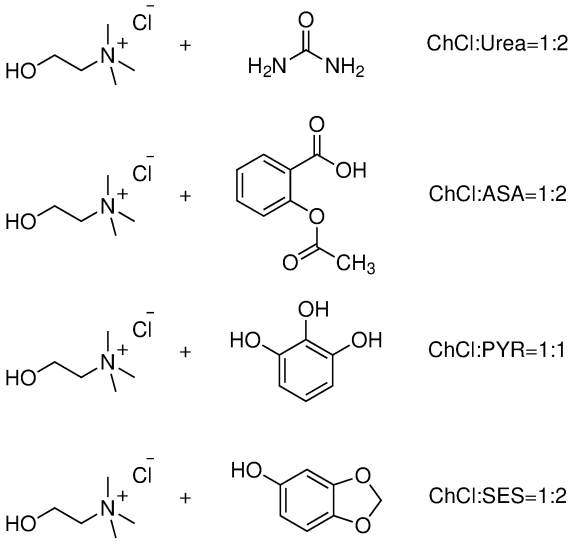

Figure 1: Schematic molecular structures of the DESs investigated in this work. From the top to the bottom the structures of the following DESs are reported: mixtures of choline chloride (ChCl) and urea, acetylsalicylic acid (ASA), pyrogallol (PYR) or sesamol (SES).

nificant environmental health concern as it is released into the environment as a toxic pollutant through a number of natural and anthropogenic cycles. One of the main sources of environmental pollution by mercury is from fossil fuels, either during coal combustion or by emission from natural gas.[25] Natural gas typically contains mercury in either elemental form or as mercuric halides (mostly $HgCl_2$) or organic mercury compounds.[26, 27] Beyond mercury health and safety risks for the biosphere, mercury is also a major problem in oil and gas processing units as it deposits in the cryogenic units by forming amalgams with different metals that lead to equipment degradation, and it also poisons many catalysts. For these reasons, it is highly desirable to develop an efficient mercury removal process [25, 27] and a promising new technology using DESs has been recently proposed.[26]

All of the above mentioned issues point to the importance of a detailed knowledge of DES-metal interactions. The speciation of metals in DESs is known to control key aspects of metal processing and it is therefore fundamental to understand if and how metal oxides and salts dissolve in DES and which species are formed inside the mixtures. Metal solvation in DESs is still poorly understood because of the complexity of the interactions between the metal and DES costituents and one key experimental technique that can furnish useful information about these systems is the X-ray absorption spectroscopy (XAS). Due to its unique short-range sensitivity and chemical selectivity, the XAS technique is ideally suited to provide accurate structural information on the solvation complexes involving metal ions,[28, 29, 30, 31, 32, 33, 34, 35, 36, 37, 38] thus making it an invaluable tool for structural characterization of such complexes in DES solvents. XAS spectra are typically split into a low-energy region, termed XANES (X-ray absorption near-edge structure), and a region which extends from about 50 eV to more than 1000 eV above the edge, which is called EXAFS (extended X-ray absorption fine structure). While the EXAFS technique has been widely employed in the past to gain structural information on metal ions in many liquid systems [39, 32, 40, 41, 42, 43, 44, 45, 46] including DESs,[47, 48, 49] to the best of our knowledge the XANES technique has not yet been explored to investigate DES systems. The XANES spectral region is very sensitive to the structural details of the absorbing site and, in principle, an almost complete recovery of the three dimensional structure can be achieved from the experimental data. However, due to the difficult theoretical treatment of the XANES features the use of this technique on a quantitative basis has been rather restricted in the past.

Here, we use the XANES and EXAFS spectroscopies, in combination with quantum mechanical (QM) calculations on cluster models, to investigate the peculiar solvation properties of the DESs with respect to typically insoluble Hg^{2+} compounds, namely $HgCl_2$ and HgO which are known not to dissociate in any solvent. Four different DESs were prepared, all based on choline chloride (ChCl) as hydrogen bond acceptor, mixed with four different hydrogen bond donors, namely urea, acetylsalicylic acid (ASA) and sesamol (SES) in a 1:2 molar ratio and pyrogallol (PYR) in a 1:1 molar ratio. The structures of the starting molecules are shown in Fig. 1. Changes in the DES hydrogen bond donor can have a strong impact on the solvation properties of the metal ion. As an example, it has been shown that the solubility of metal oxides in DESs is largely dependent on the selected hydrogen bond donor.[13] Abbott et al. determined the solubility of oxides involving first row transition metals Ti through Zn in three DESs based on choline chloride and urea, malonic acid, or ethylene glycol and the highest solubilities were found when carboxylic acids were used, suggesting that the presence of protons could act as oxide acceptors and change the metal complex.[13, 14] In the present work, HgO was observed to dissociate only in the ChCl-ASA DES, i.e. the only one with a sufficiently acid proton coming from the carboxylic moiety. By using fast atom bombardment mass spectrometry (FAB-MS) the complexes formed by the metal ions could be identified for some of the investigated DESs, corresponding predominantly to anionic chlorometalate species of the form MCl_x^{y-} with x=2,3.[13] However, the entire composition of the metal solvation shell and the possible presence of other ligands than chloride could not be determined since FAB-MS rarely detects acids, amides and alchools cordinated to the metal ion.[13] Only in the case of ZnO dissolved in 1:2 ChCl/urea, by using electrospray mass spectrometry a signal compatible with the existence of a [ZnClO·urea] complex was obtained, suggesting that the oxygen atom remained attached to the metal center and urea acted as a ligand.[12] Conversely, when $ZnCl_2$ was dissolved in the same solvent, only anionic chlorometalate species were observed.[12] In an EXAFS investigation of metal chloride salts in DESs, it was found that all of the investigated M^{2+} metal ions, with the exception of Ni^{2+}, formed $[MCl_4]^{2-}$ complexes in diol-based DESs,[48] while in DESs containing urea either pure chloro or chloro-oxo coordination was observed.[48] On the other hand, an EXAFS analysis of silver speciation showed that solutions of $AgNO_3$ and AgCl in 1:2 ChCl:ethylene glycol exhibited an almost identical

EXAFS signal,[47] indicating that nitrate ligands were removed from the metal ion and replaced by chloride, while a different EXAFS spectrum was obtained when Ag_2O was used as a silver source, pointing to the presence of some oxygen based ligands, probably hydroxide, in the Ag^+ first solvation shell.[47]
As far as the Hg^{2+} ion is concerned, a very short (60 ps) first principle molecular dynamics simulation was carried out on a concentrated mixture of $HgCl_2$ in 1:2 ChCl/urea.[26] However, starting from different initial conditions different Hg-Cl radial distribution functions were obtained, so that no reliable information on the structure of the Hg^{2+} solvation complex formed in the DES could be retrieved.[26] Previous investigations of the hydration properties of $HgCl_2$ salt found that the molecule does not dissociate in water: according to a DFT theoretical study, Hg^{2+} coordinates three water molecules in a trigonal bypiramidal geometry,[50] while a Monte Carlo simulation using MP2-derived interaction potentials found a peculiar coordination resembling a hydrophobic solute, with an intermittent binding of one, two or three water molecules to the $HgCl_2$ molecule.[51]

2. Methods

2.1. X-ray Absorption Measurements

HgO, $HgCl_2$, ChCl, SES, urea, ASA and PYR, with a purity grade greater than 98%, were purchased from Aldrich-Fluka-Sigma S.r.l. (Milan, Italy). ChCl was dried in a muffle oven at 90 °C for 16 h to remove traces of water. ChCl-SES (1:2), ChCl-ASA (1:2), ChCl-Urea (1:2) and ChCl-PYR (1:1) were prepared by mixing the pure components and heating until homogeneous and transparent liquids were obtained.[52] The proper amount of HgO and $HgCl_2$ was dissolved into 2 mL of each solvent to obtain 0.1 M solutions. Hg L_3-edge XAS spectra of the DES solutions were collected at the 11.1 beamline of the Elettra Synchrotron in transmission mode. Cells with Kapton windows were filled with the sample and kept under nitrogen flux during data acquisition to avoid contact with the moisture of the air. All measures were performed with a Si(111) double crystal monochromator, while the storage ring was operating at 2 GeV with a beam current kept between 300 and 200 mA. Three spectra were recorded and averaged for each sample.

2.2. XANES data analysis

The XANES data analysis was carried out with the MXAN code in the framework of the full multiple scattering scheme.[53] The MXAN method is based on the muffin tin (MT) approximation for the shape of the potential and uses a complex optical potential, based on the local density approximation of the self-energy of the excited photoelectron. The MT radii used in the fitting procedures are 1.6 and 0.9 Å for mercury and chlorine, respectively. The self-energy is calculated in the framework of the Hedin-Lundqvist scheme.[54] To avoid the relevant overdamping at low energies, MXAN uses a phenomenological approach to calculate the inelastic losses on the basis of a convolution of the theoretical spectrum. This calculation uses only the real part of the HL potential, with a suitable Lorentzian function having an energy-dependent width of the form $\Gamma_{tot}(E)=\Gamma_c+\Gamma_{mfp}(E)$. The constant part, Γ_c, includes the core hole lifetime, while the energy-dependent term, $\Gamma_{mfp}(E)$, represents all the intrinsic and extrinsic inelastic processes. The $\Gamma_{mfp}(E)$ function is zero below an onset energy, E_s (which in extended systems corresponds to the plasmon excitation energy), and begins to increase from a value, A_s, following the universal functional form of the mean free path in solids. Both the onset energy E_s and the jump A_s are introduced in the $\Gamma_{tot}(E)$ function via an arctangent functional to avoid discontinuities and to simulate the electron-hole pair excitations. Their numerical values are derived at each computational step (i.e., for each geometric configuration) on the basis of a Monte Carlo fit. The experimental resolution is taken into account by a Gaussian convolution.

The minimization procedures have been carried out by testing different coordination models in which the Hg-Cl distances were optimized, while the geometry of the complex was kept fixed. Least-squares fits of the experimental data in the space of the structural and non-structural parameters were carried out by minimizing the residual function, R_{sq}, defined as:

$$R_{sq} = \frac{\sum_{i=1}^{m} w_i (y_i^{th} - y_i^{exp})^2}{\varepsilon_i^2 \sum_{i=1}^{m} w_i} \quad (1)$$

where m is the number of data points, y_i^{th} and y_i^{exp} are the theoretical and experimental absorption values, respectively, ε_i is the individual error in the experimental data set, and w_i is a statistical weight. For w_i=constant=1, R_{sq} becomes the statistical χ^2 function. Here, we assumed a constant experimental error, ε=1.2%, for the whole experimental data set. Five non-structural parameters have been optimized, namely the Fermi energy level E_F, the experimental resolution Γ_{exp}, the threshold energy E_0, and the energy (E_S) and amplitude (A_S) of the plasmon.

2.3. EXAFS data analysis

The EXAFS analysis has been carried out by means of the GNXAS program and a thorough description of the theoretical framework can be found in Ref. [55]. The amplitude function $A(k, r)$ and the phase shifts $\phi(k, r)$ have been calculated by using MT potentials and advanced models for the exchange-correlation self-energy (Hedin-Lundqvist). The values of the MT radii for mercury and chlorine are the same as those used in the XANES analysis. Inelastic losses of the photoelectron in the final state have been accounted for intrinsically by using a complex potential. The imaginary part also includes a constant factor accounting for the core-hole width. The analysis of the L_3-edge EXAFS spectra of HgO in ChCl-ASA and of $HgCl_2$ in ChCl-Urea, ChCl-ASA, ChCl-SES and ChCl-PYR has been carried out by including only a single scattering Hg-Cl first-shell signal which represents the only non-negligible contribution to the total $\chi(k)$ signal. The EXAFS signal has thus been calculated by modeling the Hg-Cl first coordination shell with

a gamma-like distribution curve with mean distance R, coordination number N, standard deviation σ and asymmetry index (third cumulant divided by σ^3) $\beta = 2p^{-\frac{1}{2}}$. Least-squares fits of the EXAFS experimental data have been performed to optimize the R, σ and β parameter, while N has been kept fixed to different values. Two non-structural parameters were also minimized, namely E_0 (core ionization threshold) and S_0^2 (many body amplitude reduction factor).[55, 56]

2.4. QM calculation details

QM calculations on $[HgCl_n]^{(2-n)+}$ cluster models (n=3-5) have been carried out by means of the Gaussian16 package,[57] using the density functional theory with the B3LYP hybrid functional. In view of previous experience,[58] we have selected the pseudo-relativistic LANL2 effective potential for mercury [59] and the valence basis set previously developed in Ref. 58, whereas the chloride ions have been described by means of the aug-cc-pVTZ basis set.[60] The QM computations have been performed both in vacuum and by using the SMD solvation model developed by Truhlar and coworkers.[61] The SMx series (with x=5-8 or D) of continuum solvation models was demonstrated to provide excellent accuracy for the prediction of free energies of solvation of molecular neutral and ionic solutes in typical organic solvents [62, 63] and the SMD model was then extended to the study of ILs [61] and recently applied to DESs.[64] In general, the SMx models have been designed to be universal, meaning that they can be applied to any solvent provided that a handful of solvent descriptors are either known from measurements or can be conveniently estimated.[61] In particular, the SMD approach allows for the use of experimentally derived solvent parameters such as hydrogen-bond acidity (α), hydrogen-bond basicity (β), surface tension (γ), dielectric permittivity (ϵ), and refractive index (n) and mathematically calculated parameters such as carbon aromaticity (ϕ) and electronegative halogenicity (ψ). We have decided to perform geometry optimization of different $[HgCl_n]^{(2-n)+}$ clusters in the 1:2 ChCl/Urea DES simulating bulk solvent effects by means of SMD. Following a previous investigation where this model was used to compute the solvation free energies of aromatic sulphur compounds in several DESs including ChCl/Urea,[64] we have taken from the literature the values of experimentally derived solvent parameters for ChCl/urea, whereas the mathematically derived parameters were calculated from the molecular structure of the various DES components.[64, 65, 66, 67, 68] In particular, the following values were adopted: ϵ=12.0, n^2=2.26, α=0.27, β=0.47, γ=52.0, ϕ=0.00 and ψ =0.0625.

3. Results

3.1. XANES analysis

Since multiple-scattering effects make large contributions to the low-energy region of the absorption spectra, XANES is very sensitive to the geometric details of the absorbing site. Therefore, its quantitative analysis can provide crucial insights into the coordination structure of the photoabsorber atom that are not achievable by any other experimental technique. Fig. 2 shows the normalized XAS spectra at the Hg L_3-edge of HgO in ChCl-ASA and of $HgCl_2$ in ChCl-Urea, ChCl-ASA, ChCl-SES and ChCl-PYR. As it can be clearly seen, all of the spectra are identical independently of the DES solvent and of the nature of the dissolved species. Due to the very high sensitivity of the XANES technique towards the local structure around the photoabsorber atom, the similarity of the XAS features unambigously shows that the local coordination around the Hg^{2+} ion is the same in all of the investigated systems. Moreover, the fact that the XAS spectra of HgO and $HgCl_2$ in ChCl-ASA are identical indicates that both molecules are dissociated in the DESs and since the coordination environment seen by the Hg^{2+} ion must be the same in all the solvents, we can conclude that the Hg^{2+} first coordination shell is composed of Cl^- anions, only. The Cl^- anion is indeed the only possible ligand which is present in all of the considered systems.

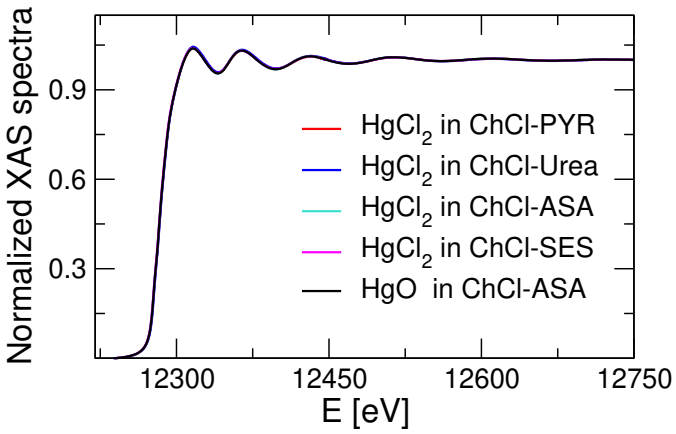

Figure 2: Normalized XAS spectra at the Hg L_3-edge of $HgCl_2$ in choline chloride-pyrogallol (ChCl-PYR), choline chloride-urea (ChCl-Urea), choline chloride-acetylsalicylic acid (ChCl-ASA) and choline chloride-sesamol (ChCl-SES) and of HgO in ChCl-ASA.

Model	N	R (Å)	E_0 (eV)	E_F (eV)	Γ_{exp} (eV)	R_{sq}
Raw spectra						
Linear	2	2.48(4)	-0.3	-4.9	3.0	3.1
Triangular planar	3	2.48(4)	-0.5	-5.9	3.3	2.4
Tetrahedral	4	2.48(4)	-0.7	-4.7	2.5	1.3
Square planar	4	2.48(4)	-0.7	-5.3	3.2	1.2
Triangular bipyramid	5	2.49(4)	-0.7	-5.1	3.2	1.4
Octahedral	6	2.48(4)	-1.1	-4.6	1.0	2.1
Deconvolved spectra						
Tetrahedral	4	2.47(4)	-2.2	-1.9	3.2	1.4
Square planar	4	2.48(4)	-2.1	-2.7	3.2	2.2
Triangular bipyramid	5	2.48(4)	-2.1	-2.1	3.3	2.3

Table 1: Structural and non-structural parameters obtained from the fitting procedures of the raw and of the deconvolved XANES experimental data of $HgCl_2$ in choline chloride-urea (ChCl-Urea) obtained by using different coordination models. R is the Hg-Cl average distance, E_0 is the threshold energy, E_F is the Fermi energy level, Γ_{exp} is the experimental resolution and R_{sq} is the residual function.

Once assessed that Cl^- anions are the only constituents of the Hg^{2+} first shell complex, we have carried out a quantitative analysis of the Hg L_3-edge XANES spectra in order to establish the coordination number and the geometry of the solva-

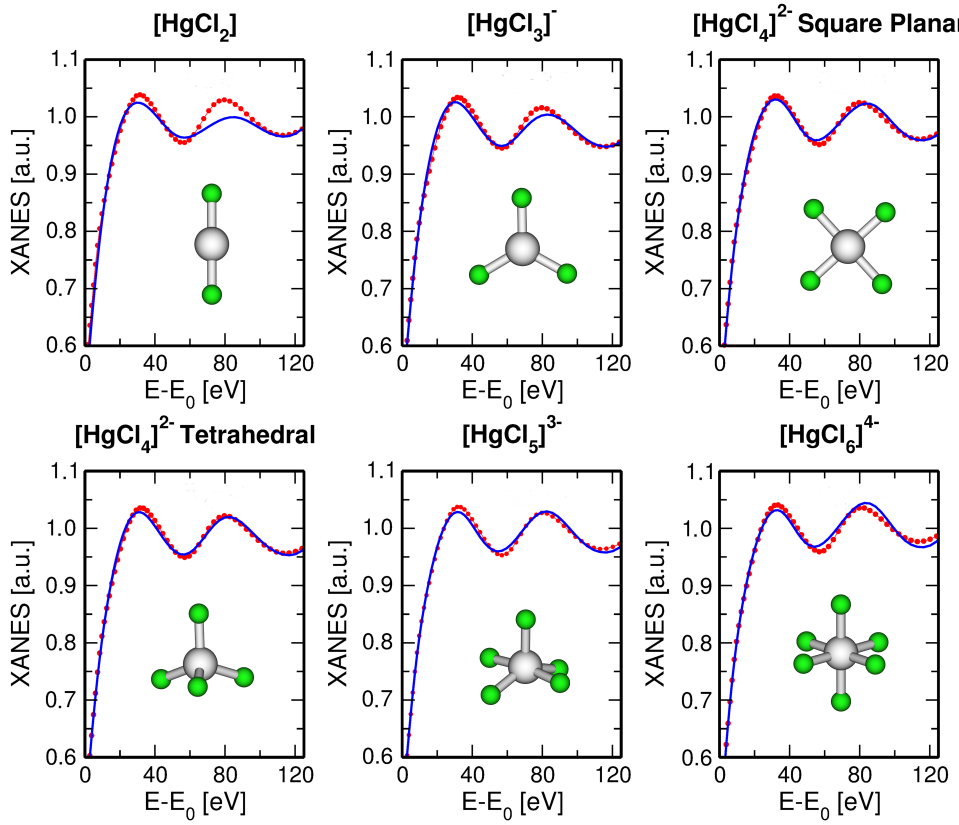

Figure 3: Comparison of the Hg L_3-edge raw XANES experimental spectrum (red points) of $HgCl_2$ in choline chloride-urea (ChCl-Urea) and the theoretical spectra (blue curves) obtained by using the following coordination models: linear $[HgCl_2]$, triangular planar $[HgCl_3]^-$, square planar and tetrahedral $[HgCl_4]^{2-}$, triangular bipyramid $[HgCl_5]^{3-}$ and octahedral $[HgCl_6]^{4-}$.

tion complex formed by Hg^{2+} in all the investigated DESs. To this end, we have performed several fitting procedures of the raw XANES experimental data by using different coordination models for the Cl^- anions surrounding Hg^{2+}. In particular, we tested the following coordination models: linear $[HgCl_2]$, triangular planar $[HgCl_3]^-$, tetrahedral and square planar $[HgCl_4]^{2-}$, triangular bipyramid $[HgCl_5]^{3-}$ and octahedral $[HgCl_6]^{4-}$. Note that the $HgCl_2$ in ChCl-Urea fits are reported as an example, but the results are identical for all the investigated systems since, as mentioned above, all of the XANES spectra are identical. In the optimization procedure the angles of the hypothesized geometry were kept fixed, while the Hg-Cl distances and the non-structural parameters were refined. The results of the fitting procedures are shown in Fig. 3, while the structural and non-structural parameters obtained from the minimization procedures are listed in Table 1, together with the corresponding R_{sq} values. As it can be clearly seen from the figure, the agreement between the experimental data and the best-fit calculation is not good for the linear $[HgCl_2]$, triangular planar $[HgCl_3]^-$ and octahedral $[HgCl_6]^{4-}$ coordination models, as also evidenced by the large values of the R_{sq} values obtained. On the basis of these results, we can exclude the existence of such geometries for the Hg^{2+} solvation complex. Conversely, a similar agreement between the experimental and theoretical XANES spectra is obtained for the tetrahedral and square planar $[HgCl_4]^{2-}$ and for the triangular bipyramid $[HgCl_5]^{3-}$ geometries. However, the differences in the R_{sq} values obtained are not significant, indicating that we are not able to discriminate among these coordination complexes. In order to overcome such ambiguity, we have resorted to apply a core-hole width deconvolution procedure to the L_3-edge raw experimental XANES spectrum of $HgCl_2$ in ChCl-Urea. When dealing with heavy elements, due to the large core hole widths of the absorbing atoms, the XANES signal is strongly broadened and the structural oscillations are smeared out from the spectra. To solve this problem it has been suggested to apply core hole width deconvolution methods to the XANES spectra that largely facilitate the detection of the spectral features.[69] It is important to stress that the complete deconvolution of the core-hole broadening would provide the real shape of the XANES region, but this is not possible due to the noise blow-up effect. As a consequence, a Gaussian filter with full width at half-maximum σ is adopted, and the minimum σ that can be used is limited by the noise blow-up effect. In a typical case where the noise level is on the order of 10^{-4} , the corresponding minimum σ value is $\sigma = \Gamma_c/3$.[70, 71] The optimal σ can be chosen on a case-by-case basis by selecting the lowest value that does not give rise to ringing artifacts in the deconvolved spectrum, and its value clearly depends on the quality of the original spectrum. The possibility to convert the Lorentzian resonance into a much narrower Gaussian peak is

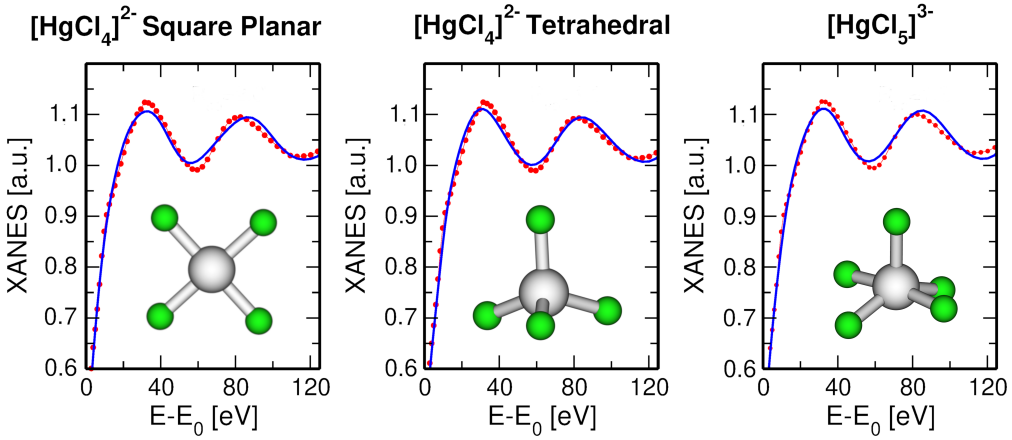

Figure 4: Comparison of the Hg L_3-edge deconvolved XANES experimental spectrum (red points) of $HgCl_2$ in choline chloride-urea (ChCl-Urea) and the theoretical spectra (blue curves) obtained by using the following coordination models: square planar and tetrahedral $[HgCl_4]^{2-}$ and triangular bipyramid $[HgCl_5]^{3-}$.

at the basis of the good results of the deconvolution procedure. In the present case, the core-hole width at the Hg L_3-edge is Γ_c = 5.5 eV and the deconvolution procedure has been carried out by deconvolving the entire Γ_c value and applying a Gaussian filter with full width at half maximum values of 1.9 eV. This value has been chosen according to the previously mentioned criterion. The experimental XANES spectrum of $HgCl_2$ in ChCl-Urea obtained by means of the deconvolution procedure is shown in Fig. 4 and, as it can be seen, after the deconvolution, the threshold region is sharpened with respect to the original spectrum, and the intensity of the structural oscillations is enhanced, with a consequent increase of the spectrum sensitivity to the chemical environment seen by the photoabsorber atom. We have thus carried out three additional fitting procedures of the deconvolved XANES spectrum by using the three coordination models that provided the best agreement with the experimental raw data, namely the tetrahedral and square planar and the triangular bipyramid coordination geometries. The optimization procedures have been carried out on the line of the previous analyses and the fitting results are shown in Fig. 4, while the optimized structural and non-structural parameters are reported in Table 1, together with the corresponding R_{sq} values. In this case, the fitting results obtained by using a tetrahedral geometry show a much better agreement with the deconvolved experimental signal than the theoretical spectra calculated for the square planar and the triangular bipyramid symmetries. From a quantitative point of view, the R_{sq} value associated with the tetrahedral best-fit result is significantly lower than the values obtained for the other two coordination models, thus showing that the Hg^{2+} ions in the investigated DESs form a first shell coordination complex composed of four Cl^- ligands arranged in a tetrahedral fashion. Note that the structural parameters obtained from the analyses of the raw and deconvolved XANES spectra are equal within the statistical errors.

3.2. EXAFS analysis

It has been shown that the MXAN analysis can be affected by systematic errors arising mostly because of the approximation used for the phenomenological broadening function Γ_{mfp}(E) that mimics the electronic damping.[72, 73] Conversely, a very accurate determination of first shell distance can be obtained by analyzing the EXAFS region of the XAS spectrum.[74, 75] For this reason, we have decided to carry out a quantitative analysis of the L_3-edge EXAFS experimental spectra of HgO in ChCl-ASA and of $HgCl_2$ in ChCl-Urea, ChCl-ASA, ChCl-SES and ChCl-PYR. In particular, we have performed least-squares fits of the EXAFS spectra in the range k = 2.5-12.2 $Å^{-1}$ by using an asymmetric shell to model the Hg-Cl distribution. The minimization procedures were applied to the whole set of structural and nonstructural parameters with the exception of the Hg-Cl first shell coordination number that has been fixed to 4 on the basis of the XANES results. Only the Hg-Cl two body theoretical signal has been considered as the Cl-Hg-Cl multiple scattering paths have been found to provide a negligible contribution. As a result the geometry of the coordination complex cannot be determined from the EXAFS analysis. The comparison between the experimental EXAFS spectra and the theoretical best-fit signals obtained for all the investigated systems is shown in Fig. 5, together with the non-phase-shift corrected Fourier transforms (FTs) of the experimental data and of the theoretical signals calculated in the range k = 2.5-10.5 $Å^{-1}$. A very good agreement between the theoretical and experimental spectra has been obtained in all cases showing the reliability of the determined structural parameters that are listed in Table 2. Note that the Hg-Cl structural parameters obtained for HgO in ChCl-ASA and of $HgCl_2$ in ChCl-Urea, ChCl-ASA, ChCl-SES and ChCl-PYR are the same within the statistical errors. Moreover, the Hg-Cl average distance is equal to the XANES determinations.

In the last step of the analysis the EXAFS experimental data have been analyzed using a Hg-Cl coordination number of 5. Additional minimization procedures have been carried out and also in this case a very good agreement between the EXAFS experimental and theoretical signals has been obtained. The best-fit structural parameters are listed in Table 2 and the Hg-Cl distances associated with the five-fold coordination model are

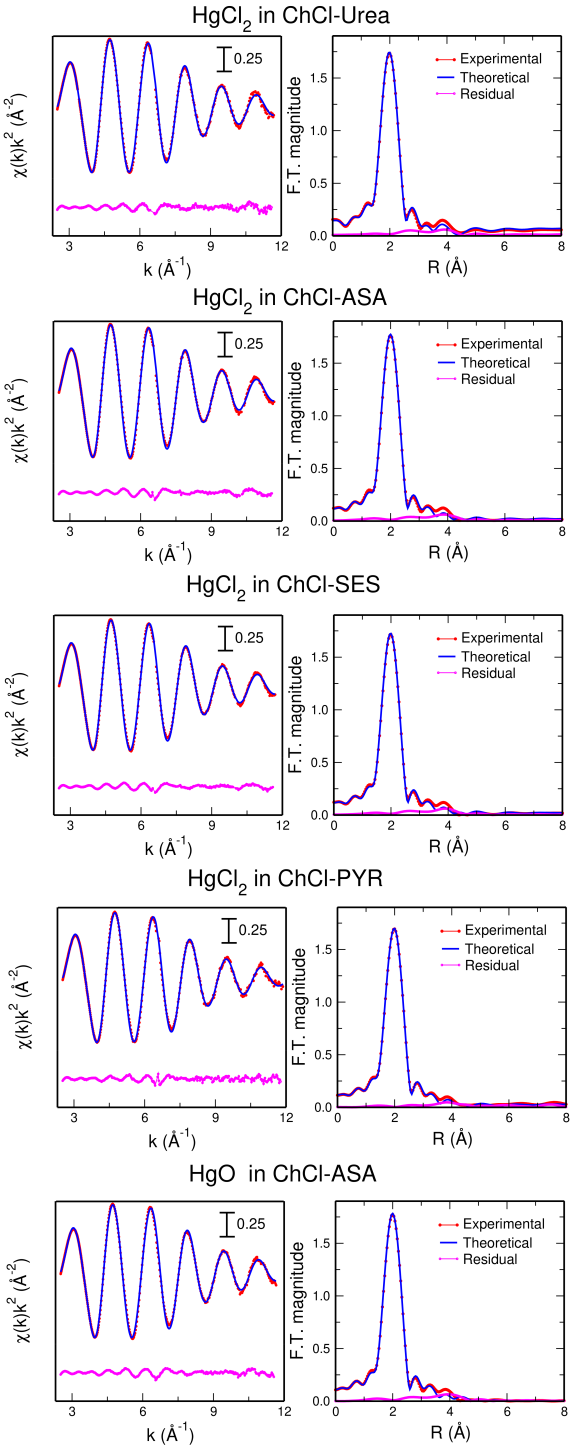

Figure 5: Left panels: comparison between the Hg L_3-edge experimental (red points) and theoretical (blu curve) EXAFS spectra of $HgCl_2$ in ChCl-Urea, ChCl-ASA, ChCl-SES and ChCl-PYR and of HgO in ChCl-ASA and corresponding residual curve (magenta line). Right panels: non-phase-shift corrected Fourier transforms of the experimental data (red points), of the theoretical signals (solid blue line) and the residual curve (magenta line).

the same as those of the four-fold cluster, while higher values of the Debye-Waller factors are obtained. It is well known that in the EXAFS analysis there is a strong correlation between

Sample	N	R (Å)	σ^2 (Å^2)	β
$HgCl_2$ in ChCl-Urea	4	2.47(1)	0.006(2)	0.1(1)
	5	2.47(1)	0.008(2)	0.1(1)
$HgCl_2$ in ChCl-ASA	4	2.47(1)	0.006(2)	0.0(1)
	5	2.47(1)	0.008(2)	0.0(1)
$HgCl_2$ in ChCl-SES	4	2.47(1)	0.006(2)	0.1(1)
	5	2.47(1)	0.007(2)	0.0(1)
$HgCl_2$ in ChCl-PYR	4	2.47(1)	0.006(2)	0.1(1)
	5	2.47(1)	0.008(2)	0.0(1)
HgO in ChCl-ASA	4	2.47(1)	0.006(2)	0.0(1)
	5	2.48(1)	0.008(2)	0.0(1)

Table 2: Best-fit parameters obtained from the analysis of the EXAFS experimental spectra for $HgCl_2$ in choline chloride-urea (ChCl-Urea), choline chloride-acetylsalicylic acid (ChCl-ASA), choline chloride-sesamol (ChCl-SES) and choline chloride-pyrogallol (ChCl-PYR) and of HgO in ChCl-ASA. N is the Hg-Cl coordination number, R is the average distance, σ^2 is the Debye-Waller factor, and β is the asymmetry parameter.

Debye-Waller factors and coordination numbers, as both parameters are related to the amplitude of the EXAFS oscillation. As a consequence, the coordination number of the Hg^{2+} solvation complex cannot be accurately determined from the EXAFS data analysis, while a very accurate determination of the Hg-Cl first shell distance can be obtained.

3.3. *QM calculations*

In order to further proceed, we have performed a comprehensive QM study of different $[HgCl_n]^{(2-n)+}$ clusters both in vacuum and simulating bulk solvent effects by means of the SMD solvation model.[61] From the similarity of the XAS spectra of $HgCl_2$ salt and HgO dissolved in all of the investigated DES systems, it was evidenced that in all cases the same atoms are present in the Hg^{2+} first solvation shell arranged in the same solvation geometry. In order to include the solvent effects in the QM calculations, we have decided to use the ChCl/urea solvent, which is in general the most studied DES. For this system, all of the experimental solvent descriptors that are required to carry out the SMD calculations are available in the literature. [64, 65, 66, 67, 68] For additional details on the solvation model see the Methods section. The XANES analysis pointed towards the existence of tetrahedral, square planar or triangular bipyramid cluster models, with the tetrahedral solvation geometry showing the best agreement with the deconvolved experimental XANES signal. We have therefore decided to carry out geometry optimizations of these three structures and the results obtained from the QM analysis are reported in Table 3. Among the three optimization procedures, only for the $[HgCl_4]^{2-}$ tetrahedral geometry a true energy minimum (all positive Hessian eigenvalues) was found, both in vacuum and in the ChCl/urea solvent simulated with the SMD model. Many attempts have been made to further optimize the $[HgCl_4]^{2-}$ square planar geometry starting from different Hg-Cl initial distances and allow-

ing all of the distances to vary, but in all cases the same stationary point was obtained with all the Cl^- ions at the same distance from the Hg^{2+} ion. The $[HgCl_4]^{2-}$ square planar structure thus represents a saddle point, with the $[HgCl_4]^{2-}$ tetrahedron minimum being at a lower energy as found both in vacuum and with the SMD solvent. As far as the $[HgCl_5]^{3-}$ cluster is concerned, if a single Hg-Cl distance is imposed in the geometry optimization procedure, a stationary point corresponding to a trigonal bipyramid geometry is found. However, this structure does not correspond to an energy minimum as negative Hessian eigenvalues have been obtained. By allowing all of the five Hg-Cl distances to vary independently from each other, the optimization procedure does not lead to any stationary points but it generates a structure where the three Cl^- ions in the triangular plane of the trigonal bipyramid remain close to Hg^{2+}, while the two apical Cl^- ions are progressively moved away from the central metal ion. This finding has prompted us to carry out an additional optimization of a $[HgCl_3]^-$ cluster model with the three Cl^- ions arranged in a triangular planar geometry. In this case true energy minima have been found both in vacuum and with the solvation model. By comparing the energy of the $[HgCl_4]^{2-}$ tetrahedral cluster to the value obtained by summing up the energy of the $[HgCl_3]^-$ optimized cluster and of the isolated Cl^- ion we find that the $[HgCl_3]^-$ structure is more stable than the $[HgCl_4]^{2-}$ one in vacuum, but the two species become isoenergetic when bulk solvent effects are taken into account through the SMD (see Table 2). Note that such a solvent induced energy variation occurs with only negligible geometry modifications. Inclusion of nonpotential energy terms (zero-point energy, thermal enthalpic, and entropic contributions) does not modify the results in an appreciable way. We can therefore conclude that the ab initio calculations are not able to discriminate between the $[HgCl_3]^-$ and $[HgCl_4]^{2-}$ tetrahedral models, but the XANES results clearly show that a $[HgCl_3]^-$ complex is not compatible with the experimental data. On the other hand, the ab initio results obtained for the $[HgCl_4]^{2-}$ tetrahedral, square planar and $[HgCl_5]^{3-}$ cluster models strongly support the experimental findings that the Hg^{2+} ion forms in DESs a complex with four chloride ions arranged in a tetrahedral geometry.

		vacuo	SMD
$[HgCl_3]^-$	R	2.52	2.59
	Energy	-1423.689	-1423.780
$[HgCl_4]^{2-}$ Tetrahedral	R	2.66	2.66
	Energy	-1883.940	-1884.188
$[HgCl_4]^{2-}$ Square Planar	R	2.69	2.72
	Energy	-1883.914	-1884.178
$[HgCl_5]^{3-}$	R	2.84	2.79
	Energy	-2344.049	-2344.571
Cl^-	Energy	-460.311	-460.408

Table 3: Energy values (au) and Hg-Cl distances R (Å) of the $[HgCl_3]^-$, $[HgCl_4]^{2-}$ and $[HgCl_5]^{3-}$ clusters obtained from the QM calculations carried out in vacuum and by using the SMD solvation model. The $[HgCl_3]^-$ and $[HgCl_4]^{2-}$ tetrahedral complexes only correspond to true energy minima (see text). The energy values of the isolated Cl^- ion are also reported.

4. Discussion and Conclusion

In this work we have investigated the solvation properties of the $HgCl_2$ salt in ChCl-Urea, ChCl-ASA, ChCl-SES and ChCl-PYR and of HgO dissolved in ChCl-ASA. The first important result we found is that both $HgCl_2$ and HgO molecules are completely dissociated in all the investigated DESs, at variance with the behaviour of $HgCl_2$ in water where such molecule does not dissociate. Moreover, the Hg^{2+} first coordination shell was shown to be composed only of Cl^- anions in all the systems, with a local structure of Cl^- ligands around Hg^{2+} which is the same independently of the DES solvent and of the nature of the dissolved species. This finding demonstrates the unique capability of these solvents to break the Hg-O and Hg-Cl bonds, cleavage that does not happen in any other solvent because of the strong covalent character of both molecules. In order to establish the coordination number and the geometry of the solvation complex formed by Hg^{2+} in the DESs we have carried out fitting procedures of the Hg L_3-edge raw XANES experimental data by using different coordination models for the Cl^- anions surrounding Hg^{2+}. On the basis of the fitting results, we could exclude the linear $[HgCl_2]$, triangular planar $[HgCl_3]^-$ and $[HgCl_6]^{4-}$ octahedral coordination models, while we were not able to discriminate among tetrahedral and square planar $[HgCl_4]^{3-}$ and the triangular bipyramid $[HgCl_5]^{3-}$ geometries. Such ambiguity has been overcome by applying a core-hole width deconvolution procedure to the L_3-edge raw experimental XANES spectrum of $HgCl_2$ in ChCl-Urea. This approach allows one to obtain an enhanced intensity of the structural oscillations with a consequent increase of the spectrum sensitivity to the chemical environment seen by the photoabsorber atom. By carrying out fitting procedures of the deconvolved XANES spectrum we have shown that the best agreement with the experimental data is obtained whith a $[HgCl_4]^{2-}$ tetrahedral coordination model. The analysis of the EXAFS spectra of $HgCl_2$ salt in ChCl-Urea, ChCl-ASA, ChCl-SES and ChCl-PYR and of HgO dissolved in ChCl-ASA allowed us to obtain a very accurate determination of the Hg-Cl first shell average distance (2.47-2.48), in agreement with the XANES determinations. Moreover, ab initio calculations of different $[HgCl_n]^{(2-n)+}$ clusters carried both in vacuum and simulating bulk solvent effects by means of the SMD solvation model strongly supported the experimental findings that the Hg^{2+} ion forms in DESs a complex with four chloride ions arranged in a tetrahedral geometry.

The existence of $[MCl_4]^{2-}$ complexes in DESs was previously suggested for other M^{2+} metal ions in diol-based DESs,[48] while in DESs containing urea either pure chloro or chloro-oxo coordination was observed.[48] However here, for the first time, by combining XANES, EXAFS and ab initio calculations we were able to unambigously determine the geometry of the Hg^{2+}

solvation complex that is, in general, a non trivial task when studying disordered systems. Moreover, the use of the XANES technique allowed us to shed light on the entire composition of the metal ion first solvation shell, which can be rarely determined by adopting other experimental techniques.[13]
The formation of a Hg^{2+} solvation complex composed only of Cl^- anions in all the ChCl-Urea, ChCl-ASA, ChCl-SES and ChCl-PYR DES indicates that Cl^- has a very strong solvation ability towards the metal ion and it forms such strong interactions with Hg^{2+} that none of the DES hydrogen bond donors is able to compete with Cl^- and act as a ligand for Hg^{2+}. These findings can represent a key step for the rational design of DESs to be used in new technologies for an efficient mercury removal process. Moreover, the strong solvation ability of Cl^- anions towards metal ions can be at the origin of the high solubility of metal oxides in chloride-based DESs, which is crucial in several important processes such as metal winning, corrosion remediation and catalyst preparation. All together our findings represent a step forward in the rationalization of the peculiar coordination properties of this new class of intriguing solvents.

Acknowledgments

We acknowledge the Elettra Syncrothron Facility for providind beam time. We acknowledge financial support from the Italian Ministry of University and Research (MIUR) through grant "PRIN 2017, 2017KKP5ZR, MOSCATo", from University of Rome La Sapienza grant n. RG11916B702B43B9. and by the CINECA supercomputing centers through the Grant IscrC_DEMETRA (n.HP10CGVY3L).

[1] A. P. Abbott, G. Frisch, J. Hartley and K. S. Ryder, *Green Chem.*, 2011, **13**, 471–481.
[2] P. Nockemann, B. Thijs, S. Pittois, J. Thoen, C. Glorieux, K. Van Hecke, L. Van Meervelt, B. Kirchner and K. Binnemans, *J. Phys. Chem. B*, 2006, **110**, 20978–20992.
[3] A. E. Visser, R. P. Swatloski, W. M. Reichert, R. Mayton, S. Sheff, A. Wierzbicki, J. H. Davis and R. D. Rogers, *Environ. Sci. Technol.*, 2002, **36**, 2523–2529.
[4] A. E. Visser, R. P. Swatloski, W. M. Reichert, R. Mayton, S. Sheff, A. Wierzbicki, J. H. Davis, Jr. and R. D. Rogers, *Chem. Commun.*, 2001, 135–136.
[5] L. C. Branco, J. N. Rosa, J. J. Moura Ramos and C. A. M. Afonso, *Chem. Eur. J.*, 2002, **8**, 3671–3677.
[6] A. P. Abbott, G. Frisch and K. S. Ryder, *Annu. Rev. Mater. Res.*, 2013, **43**, 335–358.
[7] A. P. Abbott, G. Capper, D. L. Davies, R. K. Rasheed and V. Tambyrajah, *Chem. Commun.*, 2003, 70–71.
[8] A. P. Abbott, K. E. Ttaib, G. Frisch, K. S. Ryder and D. Weston, *Phys. Chem. Chem. Phys.*, 2012, **14**, 2443–2449.
[9] S. Anggara, F. Bevan, R. C. Harris, J. M. Hartley, G. Frisch, G. R. T. Jenkin and A. P. Abbott, *Green Chem.*, 2019, **21**, 6502–6512.
[10] J. M. Rimsza and L. R. Corrales, *Comput. Theor. Chem.*, 2012, **987**, 57–61.
[11] V. Migliorati, F. Sessa and P. D'Angelo, *Chem. Phys. Lett. X*, 2019, **2**, 100001.
[12] A. P. Abbott, G. Capper, D. L. Davies, R. K. Rasheed and P. Shikotra, *Inorg. Chem.*, 2005, **44**, 6497–6499.
[13] A. P. Abbott, G. Capper, D. L. Davies, K. J. McKenzie and S. U. Obi, *J. Chem. Eng. Data*, 2006, **51**, 1280–1282.
[14] A. P. Abbott, D. Boothby, G. Capper, D. L. Davies and R. K. Rasheed, *J. Am. Chem. Soc.*, 2004, **126**, 9142–9147.
[15] N. Rodriguez Rodriguez, L. Machiels and K. Binnemans, *ACS Sustain. Chem. Eng.*, 2019, **7**, 3940–3948.
[16] M. Freemantle, *An Introduction to Ionic Liquids*, RSC Publishing, 2009.
[17] V. Migliorati, P. Ballirano, L. Gontrani and R. Caminiti, *J. Phys. Chem. B*, 2012, **116**, 2104–2113.
[18] Z. Lei, B. Chen, Y.-M. Koo and D. R. MacFarlane, *Chem. Rev.*, 2017, **117**, 6633–6635.
[19] F. Sessa, V. Migliorati, A. Serva, A. Lapi, G. Aquilanti, G. Mancini and P. D'Angelo, *Phys. Chem. Chem. Phys.*, 2018, **20**, 2662–2675.
[20] A. Serva, V. Migliorati, A. Lapi, G. Aquilanti, A. Arcovito and P. D'Angelo, *Phys. Chem. Chem. Phys.*, 2016, **18**, 16544–16554.
[21] R. L. Vekariya, *J. Mol. Liq.*, 2017, **227**, 44–60.
[22] P. D'Angelo, A. Zitolo, V. Migliorati, E. Bodo, G. Aquilanti, J. L. Hazemann, D. Testemale, G. Mancini and R. Caminiti, *J. Chem. Phys.*, 2011, **135**, 074505.
[23] J. Zhou, H. Sui, Z. Jia, Z. Yang, L. He and X. Li, *RSC Adv.*, 2018, **8**, 32832–32864.
[24] P. D'Angelo, A. Serva, G. Aquilanti, S. Pascarelli and V. Migliorati, *J. Phys. Chem. B*, 2015, **119**, 14515–14526.
[25] L. Ji, S. W. Thiel and N. G. Pinto, *Ind. Eng. Chem. Res.*, 2008, **47**, 8396–8400.
[26] S. E. E. Warrag, E. O. Fetisov, D. J. G. P. van Osch, D. B. Harwood, M. C. Kroon, J. I. Siepmann and C. J. Peters, *Ind. Eng. Chem. Res.*, 2018, **57**, 9222–9230.
[27] M. Abai, M. P. Atkins, A. Hassan, J. D. Holbrey, Y. Kuah, P. Nockemann, A. A. Oliferenko, N. V. Plechkova, S. Rafeen, A. A. Rahman, R. Ramli, S. M. Shariff, K. R. Seddon, G. Srinivasan and Y. Zou, *Dalton Trans.*, 2015, **44**, 8617–8624.
[28] V. Migliorati and P. D'Angelo, *Inorg. Chem.*, 2016, **55**, 6703–6711.
[29] A. Serva, V. Migliorati, R. Spezia and P. D'Angelo, *Chem.-Eur. J.*, 2017, **23**, 8424–8433.
[30] P. J. Merkling, A. Muñoz Páez and E. Sánchez Marcos, *J. Am. Chem. Soc.*, 2002, **124**, 10911–10920.
[31] V. Migliorati and P. D'Angelo, *RSC Adv.*, 2013, **3**, 21118–21126.
[32] P. J. Merkling, A. Muñoz Páez, J. M. Martínez, R. R. Pappalardo and E. Sánchez Marcos, *Phys. Rev. B*, 2001, **64**, 012201.
[33] V. Migliorati, A. Filipponi, A. Di Cicco, S. De Panfilis and P. D'Angelo, *Inorg. Chem.*, 2017, **56**, 14013–14022.
[34] J. L. Fulton, S. M. Kathmann, G. K. Schenter and M. Balasubramanian, *J. Phys. Chem. A*, 2009, **113**, 13976–13984.
[35] A. Tongraar, J. T-Thienprasert, S. Rujirawat and S. Limpijumnong, *Phys. Chem. Chem. Phys.*, 2010, **12**, 10876–10887.
[36] F. Sessa, V. Migliorati, A. Lapi and P. D'Angelo, *Chem. Phys. Lett.*, 2018, **706**, 311–316.
[37] L. X. Dang, G. K. Schenter, V.-A. Glezakou and J. L. Fulton, *J. Phys. Chem. B*, 2006, **110**, 23644–23654.
[38] F. Carrera, F. Torrico, D. T. Richens, A. Muñoz Páez, J. M. Martínez, R. R. Pappalardo and E. S. Marcos, *J. Phys. Chem. B*, 2007, **111**, 8223–8233.
[39] P. D'Angelo, V. Migliorati, F. Sessa, G. Mancini and I. Persson, *J. Phys. Chem. B*, 2016, **120**, 4114–4124.
[40] V. Migliorati, A. Serva, F. Sessa, A. Lapi and P. D'Angelo, *J. Phys. Chem. B*, 2018, **122**, 2779–2791.
[41] T. S. Hofer, B. R. Randolf, S. A. A. Shah, B. M. Rode and I. Persson, *Chem. Phys. Lett.*, 2007, **445**, 193–197.
[42] R. Spezia, V. Migliorati and P. D'Angelo, *J. Chem. Phys.*, 2017, **147**, 161707.
[43] H. Sakane, A. Muñoz Páez, S. Díaz-Moreno, J. M. Martínez, R. R. Pappalardo and E. Sánchez Marcos, *J. Am. Chem. Soc.*, 1998, **120**, 10397–10401.
[44] V. Migliorati, A. Caruso and P. D'Angelo, *Inorg. Chem.*, 2019, **58**, 14551–14559.
[45] T. S. Hofer, B. R. Randolf, B. M. Rode and I. Persson, *Dalton Trans.*, 2009, 1512–1515.
[46] V. Migliorati, A. Filipponi, F. Sessa, A. Lapi, A. Serva and P. D'Angelo, *Phys. Chem. Chem. Phys.*, 2019, **21**, 13058–13069.
[47] A. P. Abbott, M. Azam, G. Frisch, J. Hartley, K. S. Ryder and S. Saleem, *Phys. Chem. Chem. Phys.*, 2013, **15**, 17314–17323.
[48] J. M. Hartley, C.-M. Ip, G. C. H. Forrest, K. Singh, S. J. Gurman, K. S. Ryder, A. P. Abbott and G. Frisch, *Inorg. Chem.*, 2014, **53**, 6280–6288.
[49] T. Verdonck, P. Verpoort, J. De Strycker, A. De Cleene, D. Banerjee, P. Nockemann, R. Van Deun and K. Van Hecke, *Dalton Trans.*, 2019, **48**, 2318–2327.

[50] L. Castro, A. Dommergue, A. Renard, C. Ferrari, A. Ramirez-Solis and L. Maron, *Phys. Chem. Chem. Phys.*, 2011, **13**, 16772–16779.
[51] J. Hernández-Cobos, A. Ramrez-Sols, L. Maron and I. Ortega-Blake, *J. Chem. Phys.*, 2012, **136**, 014502.
[52] P. Tomai, A. Lippiello, P. D'Angelo, I. Persson, A. Martinelli, V. Di Lisio, R. Curini, C. Fanali and A. Gentili, *J. Chromatogr. A*, 2019, **1605**, 360329.
[53] M. Benfatto, S. Della Longa and C. R. Natoli, *J. Synchrotron Radiat.*, 2003, **10**, 51–57.
[54] L. Hedin and S. Lundqvist, *Solid State Phys.*, 1969, **23**, 1–181.
[55] A. Filipponi, A. Di Cicco and C. R. Natoli, *Phys. Rev. B*, 1995, **52**, 15122–15134.
[56] A. Filipponi and A. Di Cicco, *Phys. Rev. B*, 1995, **52**, 15135–15149.
[57] M. J. Frisch, G. W. Trucks, H. B. Schlegel, G. E. Scuseria, M. A. Robb, J. R. Cheeseman, G. Scalmani, V. Barone, G. A. Petersson, H. Nakatsuji, X. Li, M. Caricato, A. V. Marenich, J. Bloino, B. G. Janesko, R. Gomperts, B. Mennucci, H. P. Hratchian, J. V. Ortiz, A. F. Izmaylov, J. L. Sonnenberg, D. Williams-Young, F. Ding, F. Lipparini, F. Egidi, J. Goings, B. Peng, A. Petrone, T. Henderson, D. Ranasinghe, V. G. Zakrzewski, J. Gao, N. Rega, G. Zheng, W. Liang, M. Hada, M. Ehara, K. Toyota, R. Fukuda, J. Hasegawa, M. Ishida, T. Nakajima, Y. Honda, O. Kitao, H. Nakai, T. Vreven, K. Throssell, J. A. Montgomery, Jr., J. E. Peralta, F. Ogliaro, M. J. Bearpark, J. J. Heyd, E. N. Brothers, K. N. Kudin, V. N. Staroverov, T. A. Keith, R. Kobayashi, J. Normand, K. Raghavachari, A. P. Rendell, J. C. Burant, S. S. Iyengar, J. Tomasi, M. Cossi, J. M. Millam, M. Klene, C. Adamo, R. Cammi, J. W. Ochterski, R. L. Martin, K. Morokuma, O. Farkas, J. B. Foresman and D. J. Fox, *Gaussian16 Revision C.01*, 2016, Gaussian Inc. Wallingford CT.
[58] G. Chillemi, G. Mancini, N. Sanna, V. Barone, S. Della Longa, M. Benfatto, N. V. Pavel and P. D'Angelo, *J. Am. Chem. Soc.*, 2007, **129**, 5430–5436.
[59] P. J. Hay and W. R. Wadt, *J. Chem. Phys.*, 1985, **82**, 299–310.
[60] D. E. Woon and T. H. Dunning, *J. Chem. Phys.*, 1993, **98**, 1358–1371.
[61] V. S. Bernales, A. V. Marenich, R. Contreras, C. J. Cramer and D. G. Truhlar, *J. Phys. Chem. B*, 2012, **116**, 9122–9129.
[62] C. J. Cramer and D. G. Truhlar, *Acc. Chem. Res.*, 2008, **41**, 760–768.
[63] C. J. Cramer and D. G. Truhlar, *Acc. Chem. Res.*, 2009, **42**, 493–497.
[64] D. V. Wagle, H. Zhao, C. A. Deakyne and G. A. Baker, *ACS Sustain. Chem. Eng.*, 2018, **6**, 7525–7531.
[65] D. Shah and F. S. Mjalli, *Phys. Chem. Chem. Phys.*, 2014, **16**, 23900–23907.
[66] A. Pandey and S. Pandey, *J. Phys. Chem. B*, 2014, **118**, 14652–14661.
[67] G. García, S. Aparicio, R. Ullah and M. Atilhan, *Energy Fuels*, 2015, **29**, 2616–2644.
[68] A. Kadyan, K. Behera and S. Pandey, *RSC Adv.*, 2016, **6**, 29920–29930.
[69] A. Filipponi, *J. Phys. B: At. Mol. Opt. Phys.*, 2000, **33**, 2835–2846.
[70] P. D'Angelo, V. Migliorati, R. Spezia, S. De Panfilis, I. Persson and A. Zitolo, *Phys. Chem. Chem. Phys.*, 2013, **15**, 8684–8691.
[71] P. D'Angelo, V. Migliorati, I. Persson, G. Mancini and S. della Longa, *Inorg. Chem.*, 2014, **53**, 9778–9784.
[72] P. D'Angelo, M. Benfatto, S. Della Longa and N. V. Pavel, *Phys. Rev. B*, 2002, **66**, 064209.
[73] P. D'Angelo, A. Lapi, V. Migliorati, A. Arcovito, M. Benfatto, O. M. Roscioni, W. Meyer-Klaucke and S. Della Longa, *Inorg. Chem.*, 2008, **47**, 9905–9918.
[74] P. D'Angelo and V. Migliorati, *J. Phys. Chem. B*, 2015, **119**, 4061–4067.
[75] V. Migliorati, A. Serva, F. M. Terenzio and P. D'Angelo, *Inorg. Chem.*, 2017, **56**, 6214–6224.